ELECTRON BEAM STABILIZATION TEST RESULTS USING A NEURAL NETWORK HYBRID CONTROLLER AT THE AUSTRALIAN SYNCHROTRON AND LINAC COHERENT LIGHT SOURCE *

E. Meier, M.J. Morgan, School of Physics, Melbourne, Australia
S.G. Biedron, ANL, Argonne, IL 60439, USA
G. LeBlanc, Australian Synchrotron, Melbourne, Australia
J. Wu, SLAC National Laboratory, CA 94025, USA

Abstract

This paper describes the research undertaken to design an advanced control scheme for stabilization of longitudinal parameters in the FERMI@Elettra Linac. The hybrid system combines a conventional Proportional-Integral (PI) feedback controller with a feed forward using a neural network (NNET) that predicts future deviations of the beam parameters. Early experiments performed at the Australian Synchrotron showed the capability of the system to correct multi frequency energy jitter, and the advantage of combining feedback and feed forward algorithms. Further experiments conducted at the Linac Coherent Light Source (LCLS) showed that the system has the ability to simultaneously control the beam energy and bunch length. The performances of the PI and NNET were also evaluated separately for a range of jitter frequencies. The application of the system to the FERMI@Elettra Linac is also discussed.

INTRODUCTION

Because of the sensitivity of the FEL process to energy and bunch length jitter, a longitudinal feedback system is required. Based on an already existing multi-stage PID controller implemented at the Linac Coherent Light Source (LCLS), the present system aims to control longitudinal beam parameters at different stages of the machine. To compensate for the poor response of the PI algorithm at high frequencies [1], we here consider to augment it with a feed forward. Neural networks were chosen to operate this task due to their known ability to learn and adapt. Since klystrons are the main source of jitter in longitudinal dynamics when electrons are relativistic [2], the feed forward control is based on records of their phase and voltage.

CONTROLLER STRUCTURE

Figure 1 illustrates the system structure. It consists of three main blocks that are interconnected; the accelerating process, the PI algorithm, and a neural network predictor. According to Fig. 1, the accelerating process receives the set points of the "Controllables" to regulate the "Observables". In our case, the so called Controllables are the phase and voltage of the klystrons, forming the Controllable vector dC. The Observables are the energy and bunch length forming the Observable vector dO. The klystron phases and voltages are recorded and their lagged values fed into the NNET, which then computes a prediction of the deviation for the $(k+1)^{th}$ bunch in a series. The prediction is then used to compute the feed forward correction (first term in the right hand-side of Eq. (1)) , augmented by the PI correction (second and third terms in the right hand-side of Eq. (1)). The total correction can be written as:

$$dC(k+1) = -M^{-1}dO(k+1) - P_g M^{-1} dO(k) - I_g M^{-1} \sum_{l=k-R+1}^{k} dO(l), \quad (1)$$

where M is the response matrix and P_g and I_g are the proportional and integral gains of the PI feedback terms, respectively. R is the sum range of the integral term.

PRINCIPLES OF ARTIFICIAL NEURAL NETWORKS

Artificial neural networks are based on a mathematical description of biological neural networks. They consist of interconnected artificial neurons arranged in layers, as illustrated in Fig. 2 (a). They are usually arranged in input, output and hidden layers. In our case the input layer receives lagged values of the phase and voltage of a perturbed klystron, while the output layer gives the prediction of the future electron bunch energy and/or length deviation.

A single neuron, as shown in Fig. 2 (b), processes the incoming information as follows. Each of its inputs x_i has a weight w_i associated with it. The neuron then computes a weight sum $\sum_i w_i x_i$ which then goes through an activation function. The weight sum favors some inputs over others, while the activation function determines the strength the neuron fires with. Commonly used activation functions are hyperbolic tangent, sigmoid, linear and gaussian. The latter is often called a "Radial Basis Function" (RBF) because

* Work supported by Monash University, the Australian Synchrotron and in part by the Italian Ministry of University and Research under grants FIRB-RBAP045JF2 and FIRB-RBAP06AWK3 .

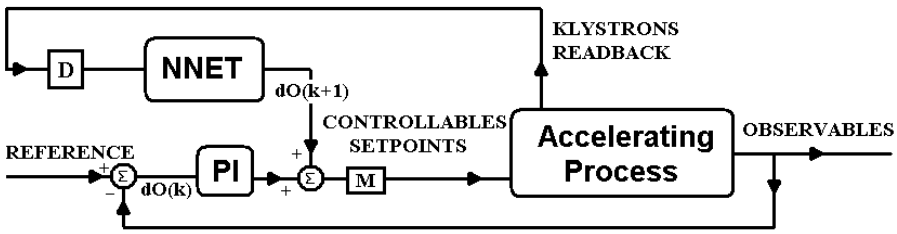

Figure 1: Control scheme used for the hybrid system. The NNET is fed with delayed values of the phase and voltage of the perturbed klystron (operator D). The predicted deviation ($dO(k+1)$) is then combined with current and past deviations of the bunches in the PI algorithm, and the sum is translated into a correction to apply using the response matrix M.

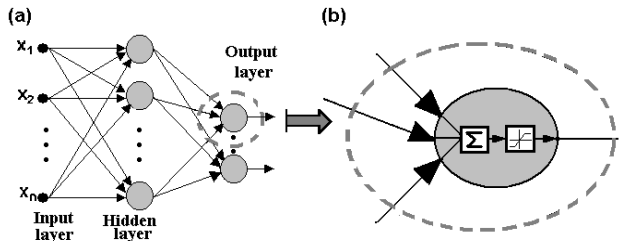

Figure 2: Schematic of an artificial neural network (a) and an individual artificial neuron (b).

of the radial nature of the gaussian function [3]. In the followings, we consider networks with hyperbolic tangent and gaussian functions. A detailed description of the procedure used to determine the appropriate number of neurons and number of lagged values can be found in [4].

To be able to make predictions, the network has to go through a training phase, where it is shown sets of inputs and desired outputs it should reproduce. Based on the error between its predictions and the desired outputs, the weights in the network are then adjusted. The process is repeated until there is either convergence of the weights or when the error between the network predictions and the desired output falls below a given limit [5]. Once the training is achieved, the NNET can be brought online.

AUSTRALIAN SYNCHROTRON LINAC STUDIES

Linac Assembly

The Australian Synchrotron Linac pictured in Fig. 3 is designed to deliver a 100 MeV electron beam to the Booster. Electrons are generated using a 90 kV electron gun. The bunching is achieved as the beam passes through a sub-harmonic pre-buncher (SPB), a primary buncher (PBU), and final buncher (FBU). Each of the two identical accelerating structures, ACC1 and ACC2 provides the beam with 50 MeV. Except for the SPB, which uses the 500 MHz master oscillator frequency, all RF structures work at 3 GHz. Two klystrons provide the RF power to the different cavities. One klystron (referred as klystron 1) powers the PBU, FBU and ACC1 and a second one (named klystron 2), powers ACC2 only. In our experiments we will impose a perturbation on klystron 1 and the correction will be applied to klystron 2.

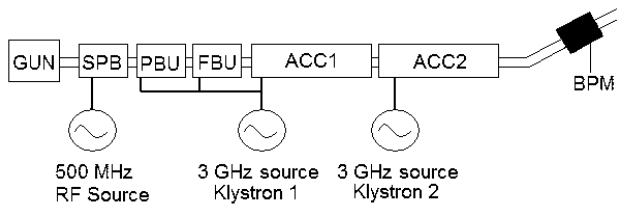

Figure 3: Australian Synchrotron Linac assembly. The bunching is achieved with the SPB, PBU and FBU sections while the ACC1 and ACC2 structures bring the beam energy to 100 MeV (figure from [6]).

Energy Stabilization Studies

Two experiments were performed. First, a hyperbolic tangent network (HTN) and a gaussian network (RBF) were trained to recognize a 3-frequency jitter induced in the first klystron phase and voltage. The three induced frequency components were 0.01 Hz, 0.02 Hz and 0.05 Hz. Results of the control based on the NNETs predictions and evaluated over 1000 pulses are given in Fig. 4. The upper plots show the record of the position deviation (left plot) and the corresponding FFT (right plot) for the induced and not corrected perturbation. The records and corresponding FFTs for the HTN and RBF controls are given in the middle and lower plots of Fig. 4, respectively. In both cases all frequency components were eliminated. The HTN however, shows a slightly better performance in terms of the remaining standard deviation. Indeed, according to Fig. 4, the remaining deviation after correction using the HTN network is 0.083 mm rms whereas it is 0.116 mm rms after correction with the RBF network. The experiment was repeated a few times and confirmed this results.

In a second experiment, the NNET system was combined to the PI algorithm. To evaluate the usefulness of the combination when the neural network is not operating optimally, we induce a change in the jitter frequency. The

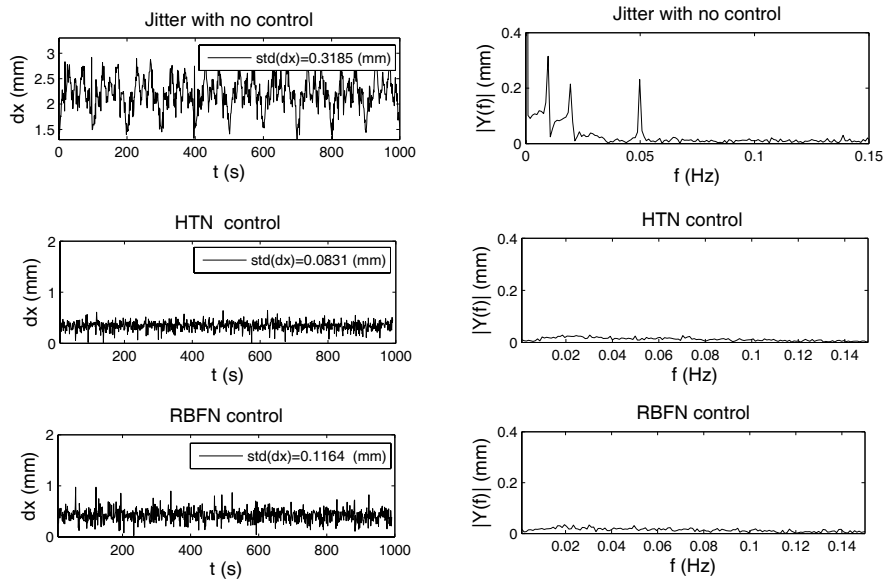

Figure 4: Online evaluation of the neural network controller. The 3-frequency perturbation (upper plots) is totally canceled by both the HTN (middle plots) and the RBF (lower plots) networks (figure from [6]).

NNET is first trained to recognize a 0.1 kV amplitude jitter at 0.04 Hz. It is then brought online to predict deviations for a 0.1 kV at 0.06 Hz jitter. For comparison, the gains of the PI algorithm were also tuned for a jitter of 0.1 kV at 0.04 Hz. Figure 5 shows the FFT for the control operated when the NNET is acting alone, when the PI is acting alone, and when both are combined. As one can see from this figure, the NNET shows better performance than the PI algorithm when both are mis-tuned. The remaining amplitude of the peak was 0.081 mm rms for the PI and 0.056 mm rms for the NNET. The combination of both decreased the amplitude of the peak further down to 0.039 mm rms, which is close to the white noise floor.

LINAC COHERENT LIGHT SOURCE STUDIES

Linac Assembly

The LCLS linac layout is illustrated in Fig. 6. Two identical accelerating structures called L0A and L0B (commonly referred to together as Linac L0) bring the beam energy to 135 MeV as it reaches the first dog leg (DL1). After the L1 and X-band sections, the beam reaches 250 MeV at the first bunch compressor (BC1) and is compressed to achieve a 250 A peak current. At the second bunch compressor (BC2) the beam attains its final 3 kA peak current at 4.3 GeV. A final section L3 will bring the final energy up to 13.64 GeV at the undulator entrance [7].

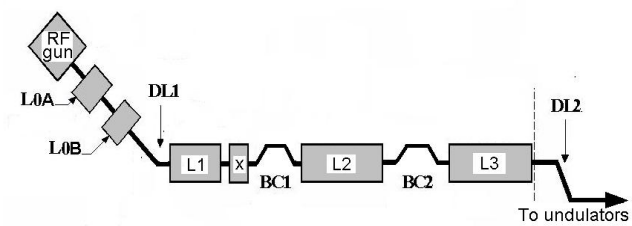

Figure 6: LCLS linac assembly. The machine main elements include four accelerating sections (L0, L1, L2 and L3) and two bunch compressors (BC1 and BC2) to deliver a 13.64 GeV and 3 kA electron beam.

Studies

The following studies aimed to pursue the work performed at the Australian Synchrotron, while testing the system for a wider frequency range. In the first experiment we demonstrate the capability of the system to simultaneously control the beam energy and bunch length. The control was operated at the second bunch compressor. Second, the performance of the PI and NNET algorithm are compared as a jitter of single and increasing frequency is applied to the phase of L1, and controlled with one of the L2 section klystrons. Third, we investigated the use of a dynamic response matrix to make the system more adaptive.

Coupled Energy and Bunch Length Control

In this experiment a 3-frequency jitter containing 0.3 Hz, 0.4 Hz and 0.6 Hz components was excited on the phase of one klystron of section L2 (named 24-1). The phase of two

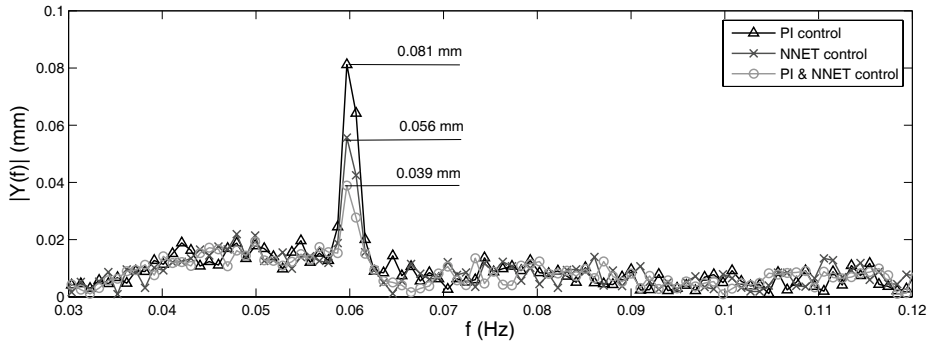

Figure 5: Comparison of the PI, NNET and coupled system. Both the PI and NNET were originally tuned to correct a 0.1 kV amplitude jitter at 0.04 Hz. The evaluation is done when the jitter frequency changes to 0.06 Hz. (figure from [6]).

downstream klystrons of section L2 (named 24-2 and 24-3) were then used as correcting actuators. The results in Fig. 7 show the FFTs of records for the beam position (upper plot) and bunch length (lower plots). The dashed curves are records of the injected perturbation (with no correction) whereas the solid curves give the records for the NNET controlled beam. As one can observe from those plots, the system was able to cancel all frequency components.

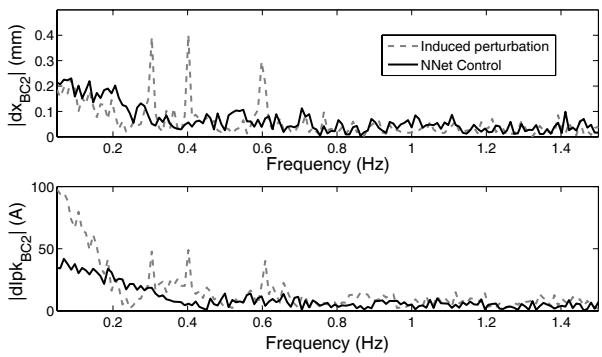

Figure 7: Simultaneous control of the beam energy and bunch length at BC2 (figure from [8]).

Comparison of PI and NNET Performances

Here we compare the performances of the PI and the NNET algorithms. For this, a single frequency jitter was injected in L1 phase and voltage, and the correcting actuator was the phase of klystron 24-2. Results are shown in Fig. 8. The remaining standard deviation of the beam position at BC2 is given as a function of the jitter frequency. Results show that above 1.5 Hz the remaining rms deviation of the beam corrected with the NNET (dashed curve) remains lower than when control is done with the PI. For each frequency the NNET was retrained and the PI gains were re-tuned. The amplitude of the initial perturbation (with no correction) was about 1 mm rms.

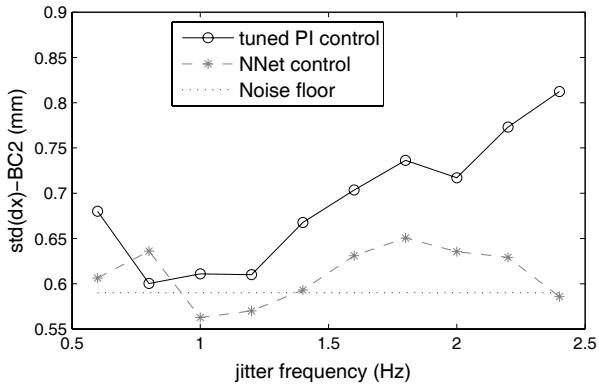

Figure 8: PI and NNET controllers performance as a function of the induced jitter frequency (figure from [8]).

Towards a More Adaptive System

Until now the klystrons settings were assumed to be constant. However, in reality these parameters will change, for example to meet different beam energy and peak current needs. When this happens, the response matrix M of the beam energy and peak current in Eq. 1 changes as well. To remedy this situation, we introduce a dynamical response matrix, with elements that are updated by a model of the machine when the klystrons settings are modified. The model includes the longitudinal equations resulting from the RF acceleration, compression and wake fields as described in [2].

To evaluate the model, we scanned the phase of klystron 24-1 and recorded the corresponding energy and bunch length deviations. Results are shown in Fig. 9 for the energy and in Fig. 10 for the peak current. As one can see from Fig. 9, the model (dashed curve) and machine (solid curve) energy responses are very close. The difference between the two curves for large deviation from the central axis (> 15 mm) is due to the non linear response of the

BPM. For the peak current, however the agreement is not as good. Despite qualitative agreement between the curves, the predicted peak current remains lower than what is produced in the machine.

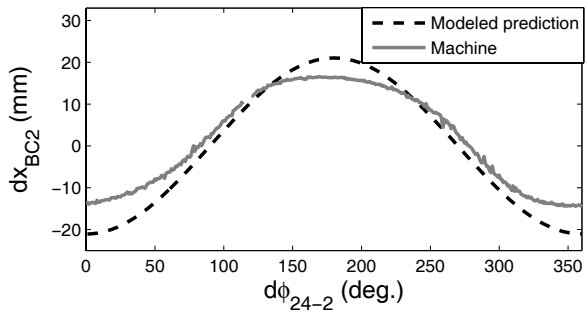

Figure 9: Machine and model predicted deviation for the beam horizontal deviation at BC2, as a function of klystron 24-1 phase. (figure from [8]).

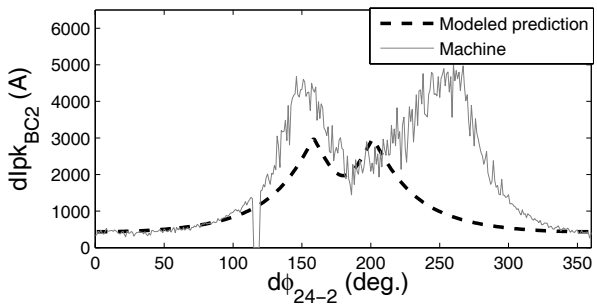

Figure 10: Machine and model predicted deviation for the bunch length at BC2, as a function of klystron 24-1 phase. (figure from [8]).

Figure 11 shows the response of the energy and peak current derived from Fig. 9 and Fig. 10. Unlike the energy response (upper curves), the modeled peak current response is not close enough to the machine response to be used in the control, and requires further development of the model.

Even with a model close to the machine response, inaccuracies can still affect the performance of the feed forward correction. In order to refine the correction when necessary, we introduce an algorithm that does slight corrections of the response matrix elements to optimize jitter reduction. In the following experiment a 0.6 Hz jitter is induced in the phase of klystron 24-1. The phase of klystron 24-2 will serve as the correcting actuator. Its initial phase setting then changed from 60° to 300°. This translates into a change in the horizontal position deviation response from 0.3 mm /° to -0.3 mm/° at BC2. To test the algorithm, the response element is set to -0.1 mm /° when the phase of klystron 24-2 is changed to 300°. The algorithm first searches for the sign of the adjustment that should be applied to the response element. A slight change is applied and the beam deviation is recorded over 200 pulses. The

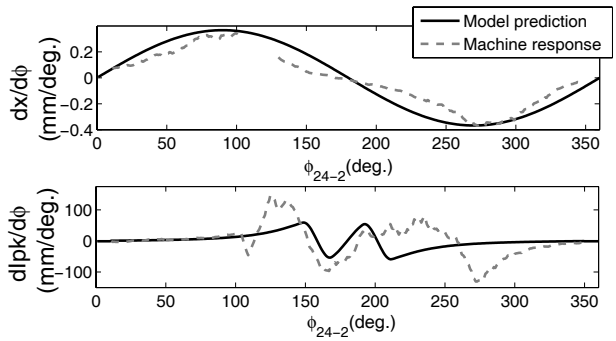

Figure 11: Comparison of the machine and model predicted response of the energy and bunch length to klystron 24-2 phase (figure from [8]).

difference in amplitude of the peak on the data FFT before and after adjustment will indicate if the sign of the correction was correctly chosen (in which case the FFT peak is reduced) or not (in which case the FFT amplitude has been increased). In the following steps the algorithm will perform corrections until the peak in the FFT is reduced to the noise floor level.

APPLICATION TO THE FERMI@ELLETRA LINAC

Linac Assembly

The machine assembly is shown in Fig. 13. Like the LCLS, it comprises of four main accelerating structures and two bunch compressors to deliver a 1.2 GeV and 800 A beam to the undulator. A laser heater is foreseen between the photo injector and the main Linac structures for Landau damping of the micro-bunching instabilities.

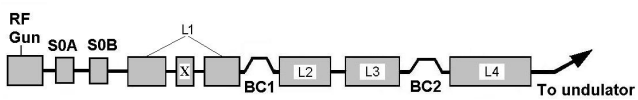

Figure 13: FERMI Linac assembly. The four main accelerating sections L1, L2, L3 and L3 provide a 1.2 GeV energy and the two bunch compressors provide a 800 A peak current.

Future Steps

Since the machine will be commissioned up to the first bunch compressor (BC1) in the first stage, we here focus on the development of the system up to that part of the machine.

In the very near future, the control system requirements and capabilities should be established. A study should also be carried out in order to determine the characteristics (amplitudes and frequencies) and sources of jitter encountered when the beam is available.

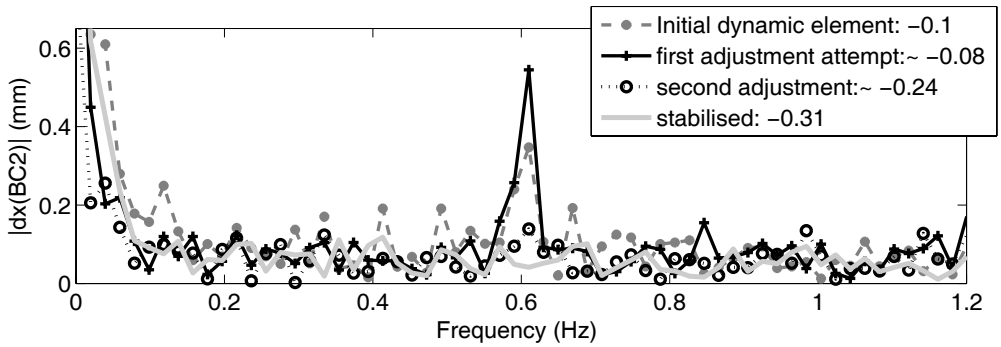

Figure 12: Energy control at BC2 using adjustments of the actuator response (figure from [8]).

A Matlab GUI will be built to operate the slow control in the first stage; i.e to correct slow drifts and periodic perturbations. It should allow the user to use different actuators for different stages of the machine, as described in [2]. This will ease the determination of a suitable Observable-Controllable configuration for the control. Since the above studies demonstrated the possibility of using the hybrid structure for the FERMI@Elettra Linac, it is envisaged that the NNET control system will be incorporated in the GUI.

CONCLUSIONS

Studies performed at the Australian Synchrotron and at the Linac Coherent Light Source showed the possibility of using neural networks to perform control of beam parameters in Linacs. The capability of the system to cancel multi-frequency jitter for energy and bunch length was demonstrated. The system was successfully complemented with a conventional PI algorithm to ensure stability of the system when the NNET does not perform optimally. The better performance of the NNET over the PI for frequencies above 1.5 Hz was also shown. A model based on longitudinal dynamics equations is being developed to build a more adaptive system, that will take klystrons settings and beam requirements into consideration.

Based on results obtained at the Australian Synchrotron and LCLS research will be pursued towards building a complementary feed forward - feedback system for the FERMI@Elettra Linac.

REFERENCES

[1] D.P. Atherton and S. Majhi, in Proceedings of the American Control Conference, 1999, pp. 3843-3847.

[2] E. Meier, FERMI@Elettra technical note, STF-TN-0815, 2008 (unpublished).

[3] J.A.K. Suykens, J.P.L. Vandewalle and B.L.R. De Moor, *Artificial Neural Networks for modelling and control of non-linear systems* (Kluwer Academic Publishers, 1997).

[4] E. Meier, S.G. Biedron, G. LeBlanc, M.J. Morgan, J. Wu, *Development of a combined feed forward-feedback system for an electron Linac*, Nucl. Instrum. Methods Phys. Res. Sect. A. Accepted for publication, August 2009.

[5] H. Demuth, M. Beale, and M. Hagan, Neural network toolbox 6 user's guide, 2008.

[6] E. Meier, S.G. Biedron, G. LeBlanc, M.J. Morgan and J. Wu, in Proceedings of the Particle Accelerator Conference, 2009.

[7] *LCLS Conceptual Design Report*, 2003.

[8] E. Meier, S.G. Biedron, G. LeBlanc, M.J. Morgan, J. Wu, *Electron beam energy and bunch length feed forward control studies using an artificial neural network at the Linac Coherent Light Source*, Nucl. Instrum. Methods Phys. Res. Sect. A. Submitted for publication, August 2009.

[9] *FERMI@Elettra Conceptual Design Report*, 2007.